LU TP 17-21
June 2017

CHAOTIC PROPERTIES OF THE DISCRETISED Φ^4 - POTENTIAL

Torbjörn Lundberg

Department of Astronomy and Theoretical Physics, Lund University

Bachelor thesis supervised by Bo Söderberg

LUND
UNIVERSITY

Abstract

Research has been conducted on integrable, Newtonian systems by B. Söderberg amongst others. Scientists uses the Hamiltonian energy landscape to simulate such systems by discretising the continuum. Non-integrable systems, however, show chaotic properties, when the Hamiltonian is not conserved along phase space trajectories. Therefore, simulations may diverge over time.

This thesis explores one particular non-integrable system, Newtonian motion in the one-dimensional scalar Φ^4-potential. The system is simulated over a lattice in a way equivalent to the discretisation of the continuum using the Leapfrog method. This system is shown to display chaotic properties, as expected from theory. Another interesting case is being put forward from the results of simulations, namely that this system displays a fractal structure. Elliptic and hyperbolic points are created along certain trajectories in phase space, around which this fractal structure seems to emerge.

Attempts were made to find a contour of convergence, inside which no trajectory diverge, but those proved fruitless. The thesis also discusses the main idea behind conserved quantities in discrete systems labelled as "shadow Hamiltonians". These are variations of the Hamiltonian and are conserved when the Hamiltonian is not.

Populärvetenskaplig sammanfattning (Swedish)

Partiklar i universum, också här på jorden, rör sig på grund av krafter som uppkommer ur egenskaper hos materien runt om oss. Föremål som fotbollar, löv och cyklister faller till marken på grund av gravitation, egenskapen att materia attraherar genom att ha en massa. Stålfjädrar kan dra ihop och trycka isär föremål på grund av krafter i materialet.

Dessa krafter kommer ur potentialer som dikterar hur mycket energi ett föremål har i en viss punkt. Dessa potentialer kan se väldigt olika ut. Ju längre bort från jorden en himlakropp befinner sig, desto mindre påverkar jordens gravitationsfält denna, medan ett föremål på en fjäder dras kraftigare in mot fjädern, ju längre utsträckt denna är.

Forskare som vill konstruera modeller för partikelrörelser måste ta hänsyn till alla dessa krafter och hitta noggranna sätt att simulera rörelser i olika potentialer. En dator måste dela upp problemet som simuleras i korta steg, och forskare måste då hitta simuleringsmetoder som ger minimal avvikelse.

I den här rapporten undersöks en särskild potential, den så kallade Φ^4-potentialen som ser ut som en djup grop med en liten kulle i botten. Denna potential visar sig ge upphov till kaotisk rörelse, d.v.s. rörelsemönster som inte går att förutsäga på samma sätt som exempelvis kastbanan för en boll i en gravitationspotential.

I undersökningen av denna potential har världen som rörelser sker i delats upp på ett speciellt sätt (diskretiseras) så att en dator kan utföra beräkningar på systemet. Den uppdelning som har gjorts resulterar i att speciella punkter, cykelpunkter, bildas enligt ett visst mönster, en fraktal. En fraktal innebär att då systemet plottas med högre upplösning, så liknar det sig själv även om bilden zoomas in. Detta är inte helt väntat och är av intresse för att bättre förstå system av den här sorten, som utvecklar sig enligt Φ^4-potentialen.

Contents

List of Figures

1 Introduction

Commonly, science is about investigating patterns. The investigation might be the uncovering of structural patterns throughout cities or behavioral patterns in human populations. In nature, reoccurring phenomena, patterns, appear in many different ways and forms. One example being the spiral pattern in Sunflowers, with its intriguing connection to the Fibonacci series [8]. Yet other species-specific patterns are found in the structural growth of branches and leaves of plants. Fundamentally, patterns in living organisms can be attributed to the specific chemical reactions taking place in the assemblage and throughout the life of said life form. The investigation of pattern generation has gained some tradition in the scientific community where, amongst others, B. Söderberg has investigated potential models for the transport of the plant hormone auxin [5]. This particular hormone is thought to be involved in the particularly interesting structure of a pine cone, which also shows a spiral structure related to the Fibonacci series [9].

Researchers as early as Alan Turing [9] have been interested in describing, mathematically, systems of particles (for example auxin) that are capable of generating patterns, since such systems apparently are present in nature. It is custom to label systems with particles able to both diffuse and react with surrounding particles: *reaction-diffusion systems*.

Several researchers at Lund University including A. Svensson [7], N. Blomberg [2], B. Söderberg [6] and N. Hermansson Truedsson [9] have been studying the ability for reaction-diffusion (RD) systems to produce patterns. They have concluded that conservative systems, i.e. such systems containing some conserved quantity, produces smooth periodic or quasi-periodic patterns [9]. It might, however, be interesting to have a closer look at systems closely related to conservative systems and highlight some differences and similarities.

The system to be investigated in this thesis is the Newtonian system governed by the one-dimensional scalar Φ^4-potential. This system gives rise to chaotic behaviour (Sec. 3.4.1) in a phase space defined in this report. Since this potential, generalised to three spatial dimensions, is present in the Higgs mechanism, both interesting and useful insights could be gained from the following analysis.

2 The mathematical starting point

In this section, the work known prior to this thesis is presented [6]. It is shown in condensed form and primarily introduces fundamental concepts, required for further analysis. For a more general formulation of reaction-diffusion (RD) system analysis, see [9].

2.1 Mathematical fundamentals of RD systems

This report is, in its core, heavily dependent on the same fundamental mathematical description used as a basis for the bachelor thesis by N. Hermansson Truedsson [9]. However,

for context, that mathematical foundation is presented in summary in this section together with material presented in appendices.

2.1.1 Reaction-diffusion equation

Any RD system may be described by a diffusion equation, modified in such a way to account for any reaction mechanisms. The generalised diffusion equation for a function $u = u(\mathbf{x}, t)$, with n-dimensional position vector $\mathbf{x}$ and t is time, is

$$\frac{\partial u}{\partial t} = D\nabla^2 u, \tag{2.1}$$

where the Laplace operator $\nabla^2 = \sum_{i=1}^{n} \frac{\partial^2}{\partial x_i^2}$. u may describe the concentration of a certain type of molecule at any particular point. Without loss of generality, the diffusion constant D may be set to 1.

Equation 2.1 takes into account any change of u in time dependent on the spatial distribution and dictates the diffusion for values of u. In order to account for reactions that affects the value of u, for example molecules reacting to increase the concentration of a substance at $(\mathbf{x}, t)$, a source term may be added to describe such reaction mechanisms:

$$\frac{\partial u}{\partial t} = \nabla^2 u + F(u), \tag{2.2}$$

with some, so far, arbitrary function $F(u)$ (consistent with dimension analysis) suitable for any particular RD system.

u could potentially display static patterns, i.e. patterns in space that do not change over time. That could especially arise from molecular concentrations. Therefore, patterns of interest to this thesis are constant in time, resulting in the partial derivative of u with respect to time to vanish in Eq.(2.2). Patterns in time, for example oscillations in a concentration of molecules, are not being discussed further on. RD systems that give rise to patterns should therefore in the continuous space fulfill the following equation:

$$\nabla^2 u + F(u) = 0. \tag{2.3}$$

The one-dimensional case of Eq.(2.3) is

$$u'' + F(u) = 0, \tag{2.4}$$

with u'' denoting the second order derivative of u with respect to x. An obvious case of the above equation would be Newtonian motion in one dimension with $F(u) \propto -V'(u)$, the derivative of some potential. For such classical motion, the total energy is conserved.

According to appendix A, the one dimensional corresponding relation to Eq.(2.3) for a spatial lattice, becomes, for small spatial separation of lattice points

$$u_+ + u_- - f(u) = 0. \tag{2.5}$$

Here $f(u) = 2u + \epsilon^2 g(u)$, so far for any $g(u)$. With u being the value at any lattice point, u_+, u_- would be the immediate surroundings of u, i.e the neighboring lattice points in the forward (u_+) and backward (u_-) direction along the spatial axis (see appendix A). Eq.(2.5) dictates the distribution of u in space and is labelled: *the equation of motion*, abbreviated EoM. This is not an equation of motion in the dynamic sense, since u is assumed to be time independent, but the equation of motion describe level curves in the phase space discussed in section 2.1.2.

2.1.2 Conserved quantities

As stated in the bachelor report by Hermansson Truedsson [9], B. Söderberg found a family of functions $f(u)$ allowing for conserved quantities in space, in one-dimensional RD systems. Constructing a map T_2 ([9]), using Eq.(2.5) and by defining $t \mathrel{\widehat{=}} u_-$, Hermansson Truedsson arrived at

$$T_2 : \begin{cases} u_+ &= f(u) - t, \\ t_+ &= u. \end{cases} \tag{2.6}$$

This is a discrete representation of a Hamiltonian system, with a phase space spanned by (u_+, u) or (u, u_-). Trajectories in such phase space represent static patterns since u is assumed to be time independent. Any possible conserved quantity in such system must be conserved along spatial trajectories. That is to require, for a given function $f(u)$, that there exists a quantity, commonly labeled H, that fulfills for any lattice points on a trajectory

$$H(u_+, u) = H(u, u_-) = H(u_-, u), \tag{2.7}$$

where the second equality imposes symmetry with respect to space reversal in u, u_-.

2.1.3 Characteristics of the phase space

For the phase space spanned by (u, u_-), Hermansson Truedsson relay information about characteristics of trajectories in said phase space. In order to conserve phase space volume, which is a condition necessarily following from the Jacobian of the mapping to be equal to unity, the expectance is that all fixed points (section 3.3) are saddle-points (hyperbolic fixed points) or centers (elliptic fixed points) [9]. By requiring the Jacobian to be 1, dissipative systems are disregarded in the continuing discussion.

Trajectories in the phase space may be periodic, quasi-periodic or chaotic [9].

2.2 The Hamiltonian

A Newtonian system behaves according to the second order time derivative of position $\ddot{x} = G(x)$ (in one dimension), hence $\ddot{x}$ denotes the acceleration of a particle. By defining $p \mathrel{\widehat{=}} \dot{x}$ with clever rescaling of variables, the problem is reduced to a set of first order differential equations. A similar map as Eq.(2.6) is achieved, in the first order expansion

of $x(t), p(t)$ for a discrete step ϵ;

$$\begin{cases} x_+ = x + \epsilon \dot{x}, \\ p_+ = p + \epsilon \dot{p}. \end{cases} \Rightarrow \begin{cases} x_+ = x + \epsilon p, \\ p_+ = p + \epsilon G(x). \end{cases} \tag{2.8}$$

In the physical world, acceleration commonly equals the negative derivative of some potential $V(x)$, s.t in one dimension $G(x) \equiv -\mathrm{d}V/\mathrm{d}x$.

In order to increase accuracy in updating x, p after a discrete step, the Leapfrog method can be utilized [6]. Starting by taking a step of length $\epsilon/2$ in x, an intermediate value $x_{1/2}$ is calculated. The obtained $x_{1/2}$ can be used to update p, a process followed by another half step in x. The mapping then becomes

$$\begin{cases} x_{1/2} = x + \frac{\epsilon}{2} p, \\ p_+ = p - \epsilon V'(x_{1/2}), \\ x_+ = x_{1/2} + \frac{\epsilon}{2} p_+ = x + \epsilon p - \epsilon V'(x_{1/2}), \end{cases} \tag{2.9}$$

with V' denoting the derivative of the potential with respect to x.

The classical expression for the Hamiltonian, which is usually a conserved quantity, $H(x,p) = p^2/2 + V(x)$ for some potential, may be investigated and updated according to $H(x,p) \to H(x_+, p_+) = H_+$, using obvious notation. The change in the value of the Hamiltonian, $\Delta H = H_+ - H$, is found to be

$$\Delta H = \frac{\epsilon^3}{4} p \left[\frac{p^2}{6} V'''(x) - V'(x) V''(x) \right] + \mathcal{O}(\epsilon^4). \tag{2.10}$$

The Hamiltonian is clearly not conserved along trajectories in phase space for most potentials. Derivation of this expression can be found in appendix B.

2.3 Shadow conservation

From the discrete expression of the change in the Hamiltonian, Eq.(2.10), it follows that the Hamiltonian is not generally conserved over trajectories in phase space for any potential $V(x) \propto x^n$, $n \geq 2$, in $\mathcal{O}(\epsilon^3)$. For some potentials, however, it is possible to find some conserved quantity, $\widetilde{H}$, which fulfills Eq.(2.7). One example would be the harmonic oscillator with potential $V(x) = \frac{k}{2} x^2$. With no loss of generality, the spring konstant may be taken as $k = 1$. For such potential $f(x) = 2x - \epsilon^2 V'(x) = (2 - \epsilon^2)x$. The discrete EoM of Eq.(2.5) then becomes

$$x_+ + x_- - (2 - \epsilon^2)x = 0. \tag{2.11}$$

Multiplying the above expression by $(x_+ - x_-)$ results in

$$x_+^2 - (2 - \epsilon^2) x_+ x = x_-^2 - (2 - \epsilon^2) x x_-. \tag{2.12}$$

It is straight forward to see that by adding x^2 to both sides, it is possible to construct

$$\widetilde{H}(x_+, x) = x_+^2 - (2 - \epsilon^2) x_+ x + x^2 = x^2 - (2 - \epsilon^2) x x_- + x_-^2 = \widetilde{H}(x, x_-). \tag{2.13}$$

Clearly this $\widetilde{H}$ fulfills Eq.(2.7) and is therefore a conserved quantity in phase space. It is labelled shadow Hamiltonian, a variation of the Hamiltonian, which has to be specifically constructed for any given potential.

3 Results for the Φ^4-potential

In this section, some aspects of choosing $V(x) = -\frac{k}{2}x^2 + \frac{\lambda}{4}x^4$, with $\lambda = \text{const}$, $k = 1$, and discretising the one-dimensional space, will be presented. This Φ^4-potential is interesting since generalisations of it exists within the Higgs mechanism, and also since it is not part of the family of functions found by Söderberg that allow for conserved quantities and hence chaotic behaviour is expected [6].

3.1 Discrete Hamiltonian

The discrete equivalence of the Newtonian equation of motion (EoM), $\ddot{x} = -V'(x)$, may be obtained from Eq.(2.5) using $u = x$ to describe position, in a potential s.t $g(u) = -V'(x)$, the first order derivative of V with respect to position.

On a lattice, the phase space variables x, p may be replaced by combinations of the discrete $x_i = i \cdot \epsilon$, $i = 0, 1, \ldots$ (see appendix A) and the neighboring lattice points of this x_i. A variable q, replacing the continuous variable x, may be represented by a mean value of lattice points, while p can be replaced by the change in x going from $x_- \to x$ using a step ϵ. The translation, from the continuum to the lattice, becomes

$$\begin{cases} x \to q \mathrel{\widehat{=}} \frac{x+x_-}{2}, \\ p \to p \mathrel{\widehat{=}} \frac{x-x_-}{\epsilon}. \end{cases} \tag{3.14}$$

Here and onwards, shorthand notation $x_i = x$ is being used. x therefore denotes a discrete variable unless otherwise mentioned.

The resulting Hamiltonian in the discrete formulation is

$$H(x, p) \to H\left(\frac{x + x_-}{2}, \frac{x - x_-}{\epsilon}\right). \tag{3.15}$$

It follows from Eq.(3.14) that

$$\begin{cases} q_+ \mathrel{\widehat{=}} \frac{x_+ + x}{2}, \\ p_+ \mathrel{\widehat{=}} \frac{x_+ - x}{\epsilon}. \end{cases} \tag{3.16}$$

It is clear from Eq.(3.14) that

$$x \equiv q + \frac{\epsilon}{2}p \mathrel{\widehat{=}} \widetilde{q} \tag{3.17}$$

Another identity is

$$q_+ = \frac{x_+ + x}{2} = \frac{\epsilon}{2}p_+ + q + \frac{\epsilon}{2}p = \widetilde{q} + \frac{\epsilon}{2}p_+. \tag{3.18}$$

Using Eq.(2.5), $x_+ + x_- - 2x = \epsilon^2 g(x) = -\epsilon^2 V'(x)$ and combining p_+, p results in

$$\epsilon(p_+ - p) \equiv x_+ + x_- - 2x = -\epsilon^2 V'(x) = -\epsilon^2 V'(\widetilde{q}) = -\epsilon^2 V'\Big(q + \frac{\epsilon}{2}p\Big). \tag{3.19}$$

$$\Rightarrow \quad p_+ = p - \epsilon V'\Big(q + \frac{\epsilon}{2}p\Big). \tag{3.20}$$

Collecting equations 3.17, 3.18 and 3.20 gives

$$\begin{cases} \widetilde{q} = q + \frac{\epsilon}{2}p, \\ p_+ = p - \epsilon V'(\widetilde{q}), \\ q_+ = \widetilde{q} + \frac{\epsilon}{2}p_+. \end{cases} \tag{3.21}$$

This is equivalent to the Leapfrog mapping of Eq.(2.9), and therefore must result in the same difference ΔH as in Eq.(2.10). Proof of this can be found in appendix C.

To find the difference in the Hamiltonian, ΔH, as the spatial coordinates changes according to Eq.(3.21), the derivatives of the Φ^4-potential is calculated and put into Eq.(2.10). The result is

$$\Delta H = \frac{\epsilon^3}{4} qp\left[-1 + \lambda p^2 + 4\lambda q^2 - 3\lambda^2 q^4\right] + \mathcal{O}(\epsilon^4). \tag{3.22}$$

By rescaling $q = \lambda^{-1/2}u$ and $p = \lambda^{-1/2}v$, the above expression is equivalent to

$$\Delta H = \frac{\epsilon^3}{4\lambda} uv\left[-1 + v^2 + 4u^2 - 3u^4\right] + \mathcal{O}(\epsilon^4). \tag{3.23}$$

3.2 Shadow conservation

Attempts were made by the author of this thesis to either find a similar conserved quantity, $\widetilde{H}$, for the scalar Φ^4-potential as was found for the harmonic oscillator (Sec. 2.3), or perhaps discard the possibility of such quantity. The attempts were not successful, but the initial reasoning can be found in appendix D.

3.3 Discrete phase space

Using the discrete formulation, with the map given by Eq.(2.6), trajectories in phase space (x, x_-) can be plotted. The scalar Φ^4-potential $V(x) = -\frac{1}{2}x^2 + \frac{\lambda}{4}x^4$ leads to the equation of motion (Eq.(2.5))

$$x_+ + x_- = 2x + \epsilon^2 x - \epsilon^2 \lambda x^3 = (2 + \epsilon^2)x - \epsilon^2 \lambda x^3. \tag{3.24}$$

In such a phase space, fixed points are expected. A fixed point is a stationary point in the phase space that is mapped onto itself. For a spatial fixed point $x = x^*$, a fixed point

in the phase space becomes (x^*, x^*). At a fixed point, Eq.(3.24) yields a polynomial of order three in x^*, that is

$$\begin{aligned} 2x_* &= (2+\epsilon^2)x_* - \epsilon^2\lambda x_*^3, \\ \Rightarrow \quad & x_*(1-\lambda x_*^2) = 0. \end{aligned}$$

Therefore all three solutions gives real valued fixed points, that are located in the phase space at

$$\begin{cases} (x_*, x_*)_1 = (0,0), \\ (x_*, x_*)_2 = \lambda^{-1/2}(1,1), \\ (x_*, x_*)_3 = -\lambda^{-1/2}(1,1). \end{cases} \tag{3.25}$$

All three fixed points are situated along the straight line $x = x_-$ in phase space.

3.4 Plotting static trajectories for the Φ^4-potential

In this section, plots of trajectories in the phase space (x, x_-) are presented. A number of starting points, $(x, x_-) = (x_0, x_0)$ were randomly generated, within a range around the origin, on the straight line $x = x_-$ and a number of trajectories were generated using the above discussed mapping.

In all figures, that are results of simulations, the scaling parameter λ was set to 1. There is no loss of generality in doing this since x always can be rescaled with a factor $\lambda^{-1/2}$.

Three main fixed point are expected as of Eq.(3.25) to be, $(1,1)$ and $(-1,-1)$ (elliptic) and $(0,0)$ (hyperbolic).

Some trajectories in the phase space have a rational winding number. This means that after a certain number of steps (updates according to the mapping), a new point on a trajectory, exactly returns to the position of a previous trajectory point. Such trajectory will include a limited number of points and is referred to as a *n-cycle*. n here represents the number of steps needed in order to return to a previous visited point, and is hence equal to the number of points on the n-cycle.

3.4.1 Chaotic behavior

In figure Fig. 1, the three expected fixed points can be seen in accordance with Eq.(3.25). Each colour represents a trajectory.

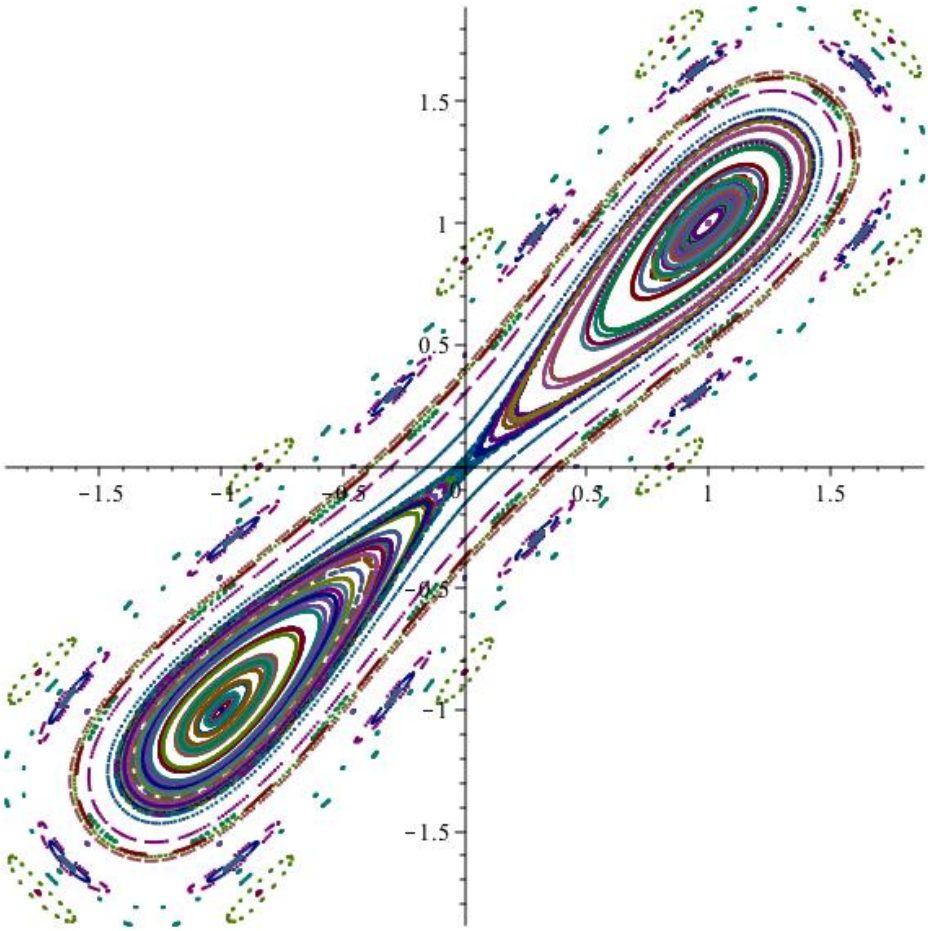

Figure 1: The figure shows trajectories in the phase space spanned by x, x_- using $\epsilon = 0.5$. Starting points of trajectories were randomly generated along the line $x = x_-$. A number of trajectories with rational winding numbers can be seen among the outmost curves. One of the most prominent trajectories with rational winding number, is the purple trajectory with points enclosed by green points of another trajectory, that forms ellipses around points of the former.

Close to the central, hyperbolic fixed point, chaos appears for increasing values of ϵ. Fig. 2 shows chaotic behavior at the origin for $\epsilon = 0.55$.

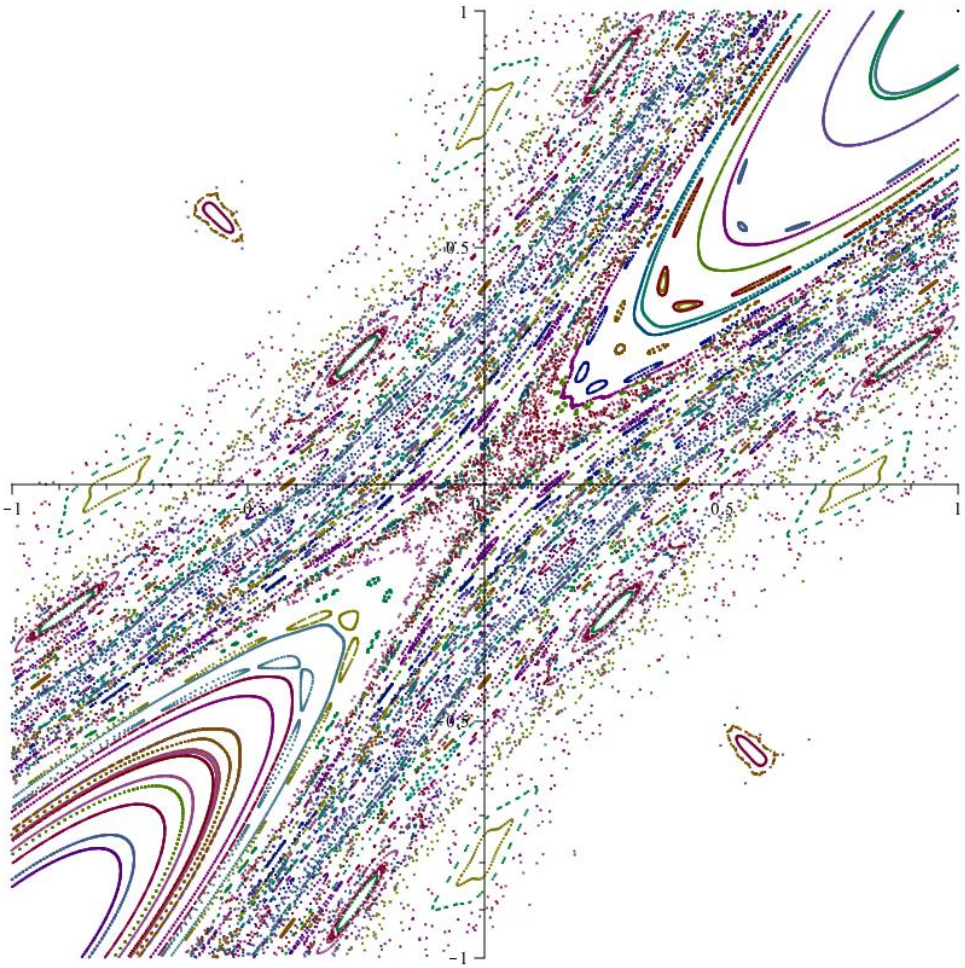

Figure 2: The figure displays chaotic behavior around the hyperbolic fixed point at the origin using $\epsilon = 0.55$. Starting points of trajectories were randomly generated along the vertical axis.

In plots above, the axes represent the phase space variables (x, x_-). If $\epsilon \to 0$, (x, x_-) will get closer and closer to the line $x = x_-$. It is possible to instead use a phase space represented by the discrete variables q, p (see Eq.(3.14)). By generating points in the phase space s.t $x = x_-$, the initial value of $p = 0$. Following Figures 8 — 13 in appendix E shows plots of the phase space in q, p for values of ϵ being 0.1, 0.3, 0.4, 0.48, 0.5 and 0.55. For increasing value of ϵ, chaotic behaviour emerges.

3.4.2 Fractal structure

Fig. 1 shows that a number of "islands" appear for certain trajectories[1]. This is the result of trajectories having a rational winding number, i.e. after a certain number of steps, a point on the trajectory returns to a point that already has been visited. A fractal structure is expected around such points [9] and in Fig. 1, elliptic fixed points can be seen. To investigate this fractal structure, and to confirm that new hyperbolic fixed points are formed between the created elliptic points (according to the Poincaré-Birkhoff theorem [9]), the following figures zoom in on the new fixed points.

To put further emphasise on the remark that a fractal structure is present [9] the elliptic point located around $(0, -0.85)$ in Fig. 1 was investigated. A more detailed simulation was conducted, with random starting points for trajectories generated on the vertical axis in a narrow range around the fixed point. Results are shown in Fig. 3.

[1] C.f. KAM-theorem by [3], [1], [4] that is commonly stated for trajectories in a phase space for an integrable Hamiltonian system. The theorem proves that if such system is disturbed by a weak, but specified, non-linear perturbation, quasi-periodic motion remains in the system.

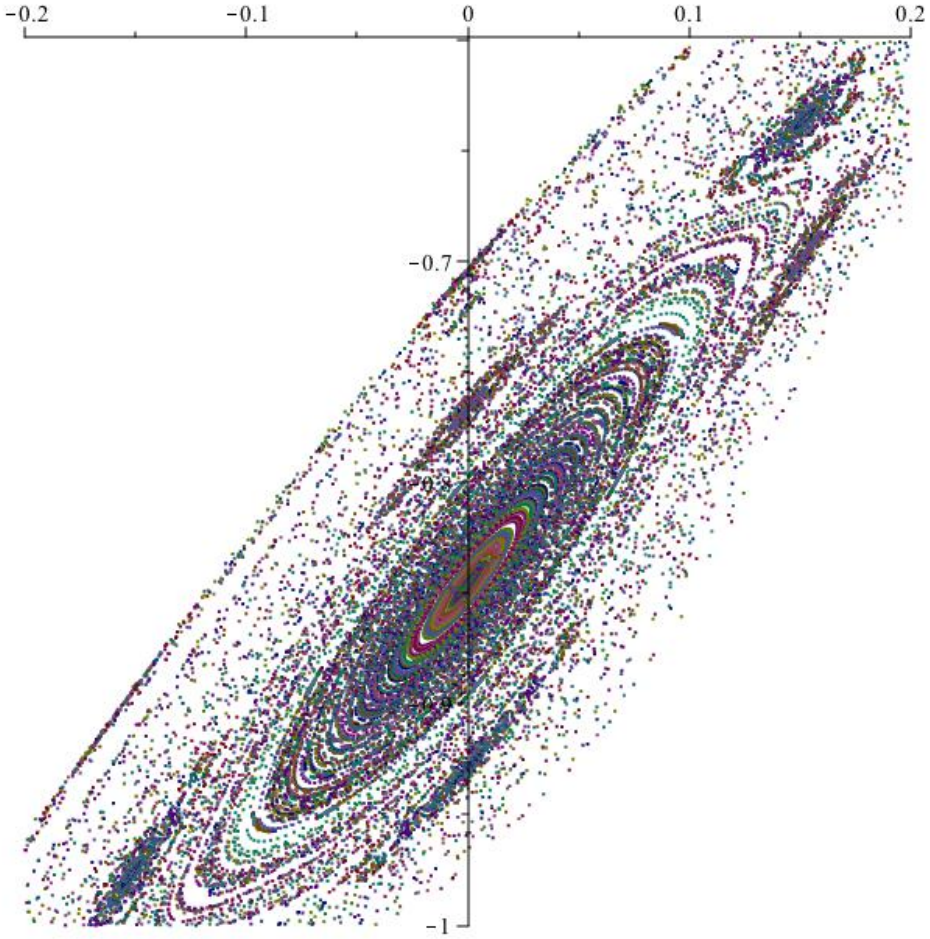

Figure 3: The figure shows trajectories around a fixed point created on a trajectory of Fig. 1, roughly located around $(0, -0.85)$. Six distinct new elliptic points are created around this centralised elliptic point, (one of which is too far down to be present in this figure). These new elliptic points are divided into two groups. Three points belonging to one trajectory, which is separate to the trajectory of the other three points. The six new points are therefore two different three-cycles around the central elliptic point. $\epsilon = 0.5$.

In Fig. 3, the six elliptic points enclosing the centralised elliptic point, are located on two different trajectories. That is of interest, since it gives information about the fractal structure, and confirmation that three elliptic points indeed are part of the same trajectory, while the others are not, is shown in Fig. 4.

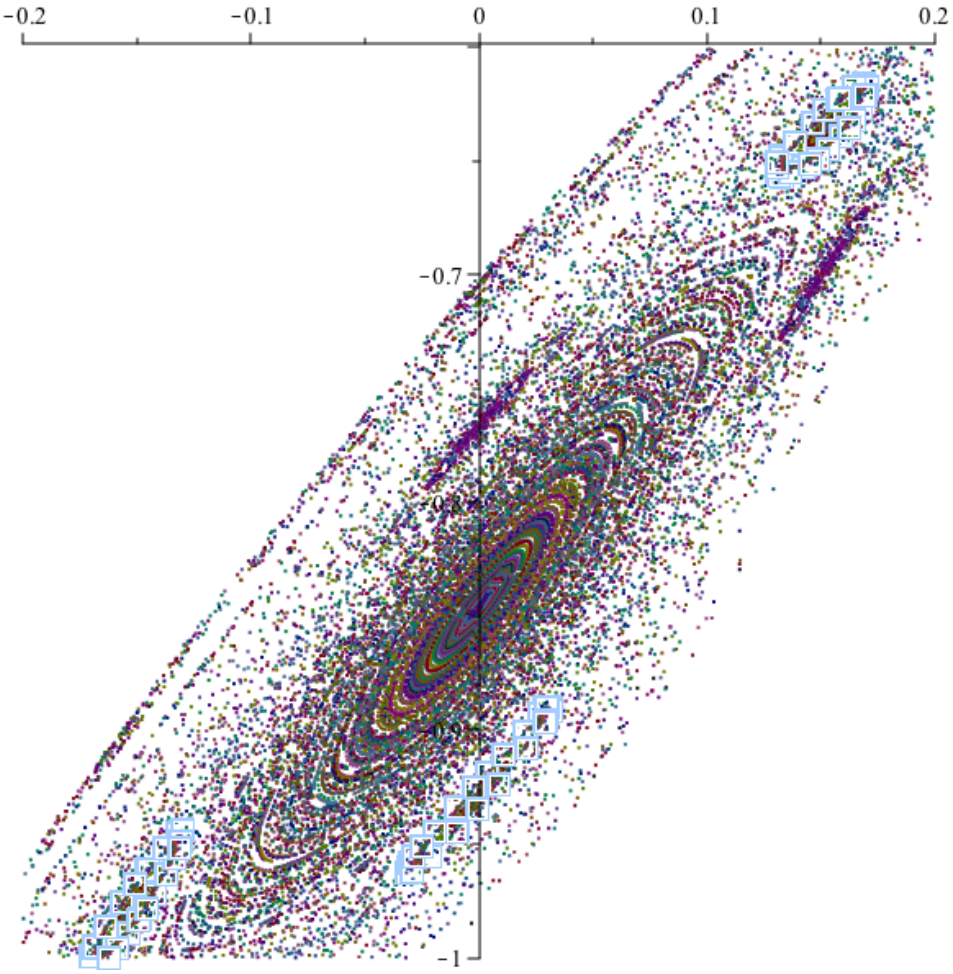

Figure 4: The figure shows trajectories around the centered elliptic point of Fig. 3, roughly located around $(0, -0.85)$. In the figure, points that lie on one trajectory are highlighted, and hence it is clear that the central elliptic point is surrounded by two 3-cycles. $\epsilon = 0.5$.

To further confirm a fractal structure, one more level of simulations was conducted, even more detailed as compared to Fig. 3. In this simulation, random starting points were generated in the vicinity of the elliptic point around $(0.15, -0.6)$, see Fig. 3 for reference. Results are displayed in Fig. 5.

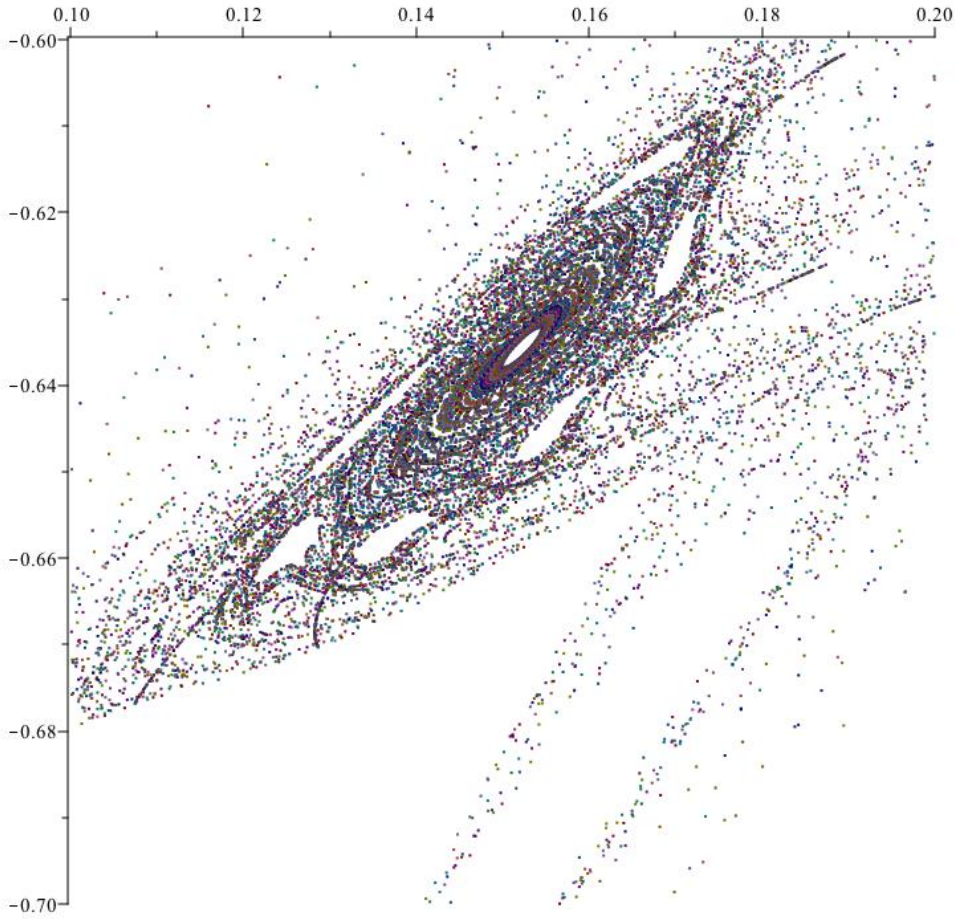

Figure 5: The figure shows trajectories in the vicinity of a fixed point created around the central elliptic point in Fig. 3. Six distinct new elliptic points are created around the centralised elliptic point. The new elliptic points all lay on the same trajectory in phase space and therefore form a six-cycle around the central elliptic point of this figure. $\epsilon = 0.5$.

To emphasise the structure of Fig. 5, Fig. 6 highlights all the points on a single trajectory, showing that the new elliptic points around the center of Fig. 5 are indeed part of the same trajectory.

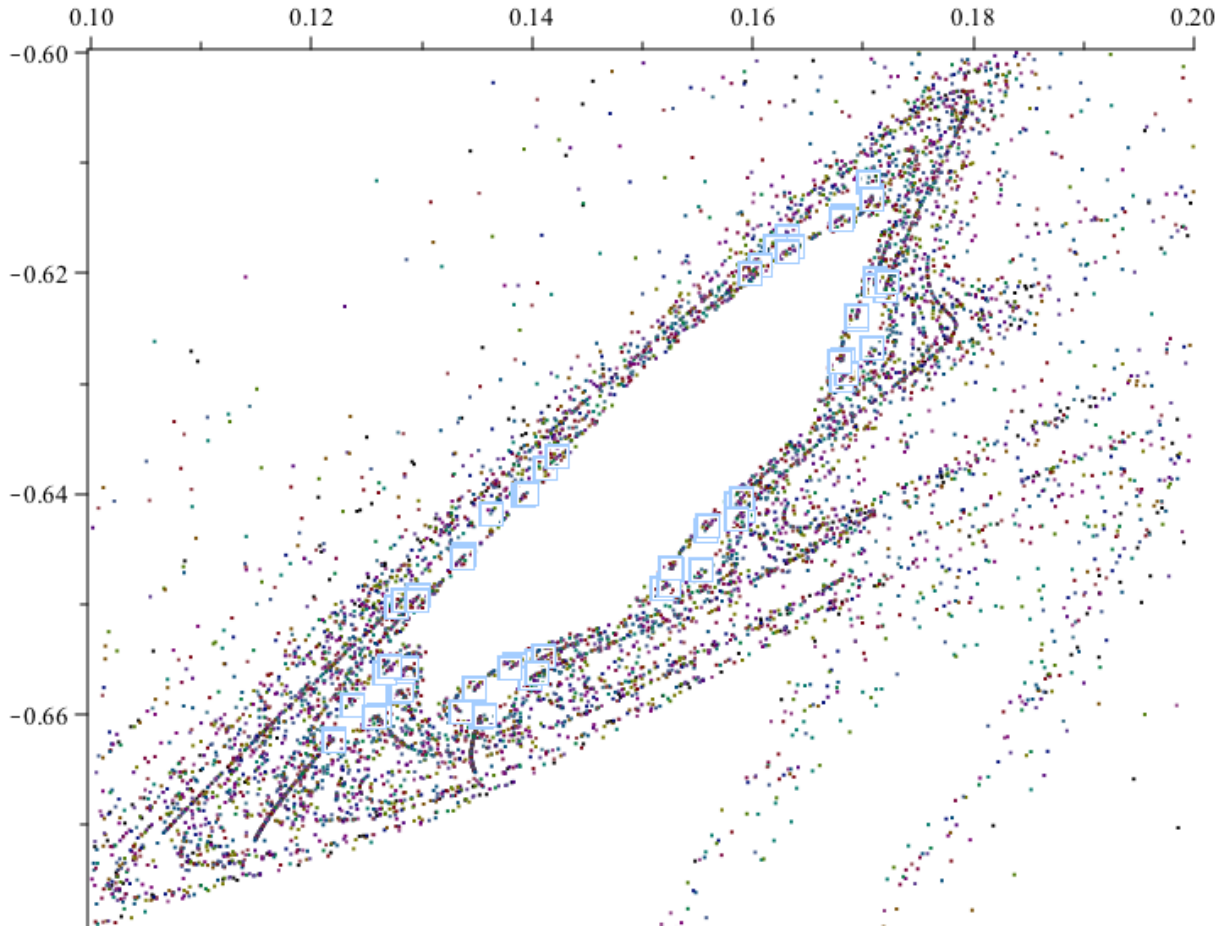

Figure 6: The figure emphasises that the six new elliptic points of Fig. 5 lay on the same trajectory, further implicating a fractal structure. $\epsilon = 0.5$.

3.4.3 Limit away from the origin

The mapping used contains a cubic term in the expression for x_+. For large values of x, far from the origin, it is therefore expected that trajectories in phase space will behave as a cubic function with respect to one axis, dominating over the second axis ($x_+ \approx -x^3$). For confirmation, a plot of typical trajectories is shown in Fig. 7, displaying results of simulations where starting points for trajectories are generated further from the origin, compared to other figures.

An attempt was made to analyse the border between third order polynomial behaviour and the more intricate patterns generated closer to the origin (c.f. Fig. 7). The idea was that there may exist a border of some shape, for which all trajectories with points inside such a border, never diverge. However, that analysis proved fruitless.

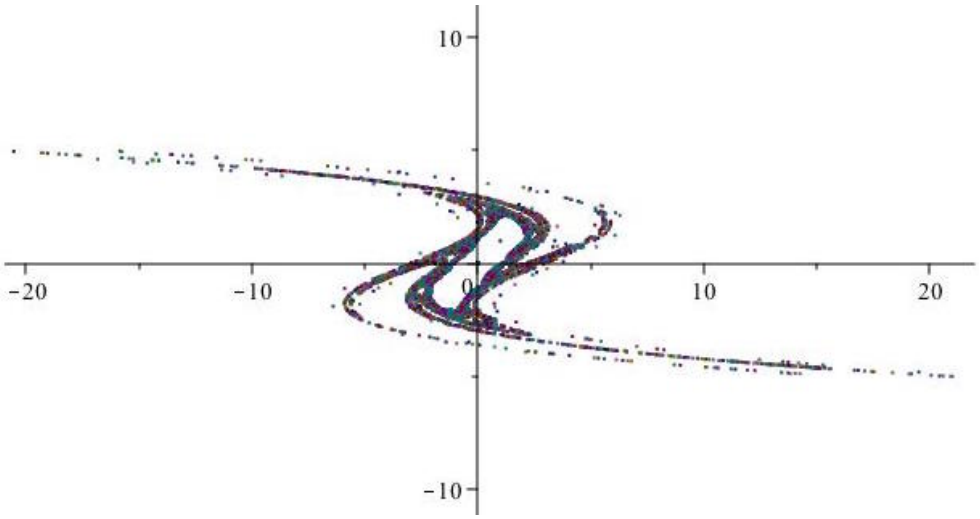

Figure 7: The figure shows the behaviour of trajectories in phase space (x, x_-), away from the origin. It is clear that trajectories takes off over a dominating axis, sensitive to sign as is expected of a cubic term. $\epsilon = 0.5$.

3.4.4 Motion patterns in the Φ^4-potential

The phase space of the scalar Φ^4-potential contains distinct regions, where different behaviour is expected. Such regions are either the surroundings of one of the two elliptic fixed points at $(1, 1)$, $(-1, -1)$ respectively, close to the hyperbolic fixed point, generating chaotic movement, or further away from those fixed points. Trajectories close to one of the elliptic fixed points form shapes resembling deformed ellipses, with n-cycles appearing, while chaos appear on trajectories close to the origin. Further from the fixed points, trajectories enclose all three points, with $n-$cycles appearing, around which chaotic behaviour can be seen for hyperbolic fixed points.

It could be of interest to plot the evolution of the spatial coordinate as $x \to x_+$, and to do so for the different regions mentioned above. Results of simulations are being presented in appendix F. For Figures 14—23, the trajectory is presented together with the value of the spatial coordinate x in generated order.

4 Summary

According to the above analysis, there are many interesting aspects of the phase space for the one-dimensional scalar Φ^4-potential. Expected chaotic behavior was found around the hyperbolic fixed point at the origin. But as seen in Figures 3 and 5, chaotic behaviour is also present around n-cyclic, hyperbolic points that appear on trajectories in the phase space. This is similar to results by Hermansson Truedsson [9].

A fractal structure around additional elliptic points was observed, to which mathematical analysis should be applied as a continuation of this project. More detailed simulations,

with results presented in Figures 3 and 5, indicated a hierarchical structure of where in the phase space new elliptical points are laid out recursively, at finer and finer resolution. The formal mathematical analysis of this aspect lies beyond the author of this report at present time, but could form an interesting basis for continued work on fractal patterns in discrete phase space.

A convergence contour around the three fixed points was not found, neither the existens of such was disproven, but the expectance is that no such shape exists in this phase space [6].

The author did not find any conserved "shadow" Hamiltonian, nor was the existence of such quantity disproven. Because of the chaotic properties of trajectories it is however reasonable to expect that there is no conserved quantity in the system.

The change in the discrete version of the Hamiltonian, over the course of a shift in space of length ϵ, was found, and the formulation in discrete variables q, p was shown to be equivalent to the continuum discretisation using the Leapfrog method.

Possible extensions of this project would be *i*) to further investigate the fractal structure of elliptic and hyperbolic points, especially the mathematics generating these points in the phase space. *ii*) Further and more rigorously investigate how the generation of elliptic and hyperbolic points around n-cycles are affected by the value of ϵ. How chaotic behaviour arises depending on ϵ would be of interest to researchers simulating such Newtonian systems where chaos is present. *iii*) To reveal further details in the discrete phase space, simulations could be conducted in a slightly different manner. Throughout this project, starting points of trajectories was exclusively generated on specific straight lines in the phase space. In order to make a more general study of the phase space, starting points could be generated randomly in a phase space region, with independent starting coordinates x, x_{-}.

A Discretised second derivative

In this section, the discretisation of the second order derivative is derived.

From the definition of the derivative

$$u'(x) = \lim_{h \to 0} \frac{u(x+h) - u(x)}{h}, \tag{A.26}$$

but using a finite step ϵ in the forwards direction, it is possible to approximate the derivative of u at x as

$$u'(x) \approx \frac{u(x+\epsilon) - u(x)}{\epsilon}. \tag{A.27}$$

The same derivative may however be approximated using a backwards step of length ϵ,

$$u'(x) \approx \frac{u(x) - u(x-\epsilon)}{\epsilon}. \tag{A.28}$$

It is possible to instead choose a symmetric approximation around x by taking a step of length $\epsilon/2$ in the forward and backward direction as

$$u'(x) \approx \frac{u(x+\epsilon/2) - u(x-\epsilon/2)}{\epsilon}. \tag{A.29}$$

Using Eq.(A.29) the second derivative $u''(x)$ may be formulated in the same manner as

$$\begin{aligned} u''(x) &\approx \frac{u'(x+\epsilon/2) - u'(x-\epsilon/2)}{\epsilon} \\ &= \frac{u(x+\epsilon) - 2u(x) + u(x-\epsilon)}{\epsilon^2}. \end{aligned}$$

In the case where the continuum is divided up into a lattice with discrete points, x_i, separated by a spatial distance of ϵ, $x_i = i \cdot \epsilon$, the second order derivative at any point, $u''(x_i)$, could be formulated in a similar manner as above. For a discretised x with $x_i - \epsilon = x_{i-1}$ and $x_i + \epsilon = x_{i+1}$, or in short hand notation $x_i = x$, $x_{i-1} = x_-$ and $x_{i+1} = x_+$,

$$u''(x) \approx \frac{u(x_+) - 2u(x) + u(x_-)}{\epsilon^2}. \tag{A.30}$$

Extending the short hand notation so that $u(x_i) = u_i = u$, $u(x_{i-1}) = u_{i-1} = u_-$ and $u(x_{i+1}) = u_{i+1} = u_+$, the above expression is equivalent to

$$u_{i+1} + u_{i-1} - 2u_i \approx \epsilon^2 u'', \quad \forall i \quad \Rightarrow \quad u_+ + u_- - 2u \approx \epsilon^2 u''. \tag{A.31}$$

If now the second derivative u'' is a function of u, $g(u)$, as hinted at in Eq.(2.3), a function $f(u)$ might be defined s.t $f(u) = 2u + \epsilon^2 g(u)$. The final expression can be written as

$$u_+ + u_- \approx f(u). \tag{A.32}$$

B Continuous Hamiltonian: in discrete steps

For a Hamiltonian

$$H(x,p) = \frac{p^2}{2} + V(x), \tag{B.1}$$

clever rescaling of variables $x(t), p(t)$ results in the dynamics

$$\begin{cases} \dot{x} = p, \\ \dot{p} = -V'(x). \end{cases} \tag{B.2}$$

Systems as Eq.(B.2) implicates that changes in x, p can be discretised using the Leapfrog method, for a step of length ϵ:

$$\begin{cases} x_{1/2} = x + \frac{\epsilon}{2} p, \\ p_+ \;\; = p - \epsilon V'(x_{1/2}), \\ x_+ \;\; = x_{1/2} + \frac{\epsilon}{2} p_+. \end{cases} \tag{B.3}$$

For values x_+, p_+, the Hamiltonian is $H(x_+, p_+) = H_+$, in obvious notation. The change in the Hamiltonian, ΔH, after one step is $H_+ - H$.

So what is H_+? Putting x_+, p_+ from Eq.(B.3) into the Hamiltonian of Eq.(B.1), results in

$$H_+ \equiv H(x_+, p_+) = \frac{1}{2} p_+^2 + V(x_+). \tag{B.4}$$

Taking

$$\frac{1}{2} p_+^2 = \frac{p^2}{2} - \epsilon p V'(x_{1/2}) + \frac{\epsilon^2}{2} \big(V'(x_{1/2})\big)^2 \tag{B.5}$$

and, using $x_+ = x + \epsilon p - \frac{\epsilon^2}{2} V'(x_{1/2})$,

$$V(x_+) = V\big(x + \epsilon p - \frac{\epsilon^2}{2} V'(x_{1/2})\big). \tag{B.6}$$

Expanding the above expression for the potential in ϵ yields

$$\begin{aligned} V(x_+) = V(x) &+ \\ &+ \epsilon p V'(x) + \\ &\quad + \frac{\epsilon^2}{2} \left[-V'(x_{1/2}) V'(x) + p^2 V''(x) \right] + \\ &\quad\quad + \frac{\epsilon^3}{2} \left[-p V'(x_{1/2}) V''(x) + \frac{p^3}{3} V'''(x) \right] + \\ &\quad\quad\quad + \mathcal{O}(\epsilon^4). \end{aligned}$$

Using Eq.(B.5) together with the above potential results in

$$\begin{aligned} H_+ = H+ \\ &+ \epsilon p \left[V'(x) - V'(x_{1/2})\right] + \\ &+ \frac{\epsilon^2}{2}\left[V'(x_{1/2})\big(V'(x_{1/2}) - V'(x)\big)\right] + \\ &+ \frac{\epsilon^3}{2} p \left[\frac{p^2}{3}V'''(x) - V'(x_{1/2})V''(x)\right] + \\ &+ \mathcal{O}(\epsilon^4). \end{aligned}$$

Expanding $V'(x_{1/2})$ to second order (anything higher will produce terms of $\mathcal{O}(\epsilon^3)$ and be multiplied by ϵ or higher order in ϵ in ΔH) results in

$$V'(x_{1/2}) = V'(x) + \frac{\epsilon}{2}pV''(x) + \frac{\epsilon^2}{8}p^2V'''(x) + \mathcal{O}(\epsilon^3). \tag{B.7}$$

This expression may be used in the equation describing ΔH, and ignoring all terms of fourth order in ϵ:

$$\Delta H = \frac{\epsilon^3}{4} p \left[\frac{p^2}{6}V'''(x) - V'(x)V''(x)\right] + \mathcal{O}(\epsilon^4). \tag{B.8}$$

C Discrete Hamiltonian: in discrete steps

Using discrete variables q, p, the translation from the continuum onto the lattice becomes

$$\begin{cases} x \to q \mathrel{\widehat{=}} \frac{x+x_-}{2}, \\ p \to p \mathrel{\widehat{=}} \frac{x-x_-}{\epsilon}, \end{cases} \tag{C.1}$$

with Hamiltonian

$$H(x,p) \to H\left(\frac{x+x_-}{2}, \frac{x-x_-}{\epsilon}\right). \tag{C.2}$$

Eq.(C.1) leads to the mapping

$$\begin{cases} \widetilde{q} = q + \frac{\epsilon}{2}p, \\ p_+ = p - \epsilon V'(\widetilde{q}), \\ q_+ = \widetilde{q} + \frac{\epsilon}{2}p_+, \end{cases} \tag{C.3}$$

and to the Hamiltonian

$$H(x_+, p_+) \to H\left(\frac{x_+ + x}{2}, \frac{x_+ - x}{\epsilon}\right) = H_+. \tag{C.4}$$

Furthermore

$$\Delta H \mathrel{\widehat{=}} H_+ - H = H\left(\frac{x_+ + x}{2}, \frac{x_+ - x}{\epsilon}\right) - H\left(\frac{x + x_-}{2}, \frac{x - x_-}{\epsilon}\right)$$
$$= \frac{(x_+ - x)^2 - (x - x_-)^2}{2\epsilon^2} + V\left(\frac{x_+ + x}{2}\right) - V\left(\frac{x + x_-}{2}\right).$$

Evaluating the first term:

From the EoM 2.5, using $u(x) = x$ and $g(u) = -V'(x)$,

$$x_+ - x = x - x_- - \epsilon^2 V'(\widetilde{q}) \tag{C.5}$$

$$\Rightarrow \quad \frac{(x_+ - x)^2 - (x - x_-)^2}{2\epsilon^2} = -\frac{x - x_-}{\epsilon}\epsilon V'(\widetilde{q}) + \frac{\epsilon^2}{2}\big(V'(\widetilde{q})\big)^2 \tag{C.6}$$

The difference in potential can be expressed, expanding the first term s.t. $V\big((x + x_-)/2\big) = V$:

$$V\left(\frac{x_+ + x}{2}\right) - V\left(\frac{x + x_-}{2}\right) = V + \left(\frac{x_+ + x}{2} - \frac{x + x_-}{2}\right)V' + \frac{1}{2}\left(\frac{x_+ + x}{2} - \frac{x + x_-}{2}\right)^2 V'' +$$
$$+ \frac{1}{6}\left(\frac{x_+ + x}{2} - \frac{x + x_-}{2}\right)^3 V''' + \ldots - V,$$

where

$$\left(\frac{x_+ + x}{2} - \frac{x + x_-}{2}\right) = \epsilon\left(\frac{x - x_-}{\epsilon} - \frac{\epsilon}{2}V'(\widetilde{q})\right). \tag{C.7}$$

$$\Rightarrow \quad V\left(\frac{x_+ + x}{2}\right) - V\left(\frac{x + x_-}{2}\right) = \epsilon\frac{x - x_-}{\epsilon}V' - \frac{\epsilon^2}{2}V'(\widetilde{q})V' + \frac{\epsilon^2}{2}\left(\frac{x - x_-}{\epsilon}\right)^2 V'' -$$
$$- \frac{\epsilon^3}{2}\frac{x - x_-}{\epsilon}V'(\widetilde{q})V'' + \frac{\epsilon^3}{6}\left(\frac{x - x_-}{\epsilon}\right)^3 V''' + \mathcal{O}(\epsilon^4).$$

Expanding

$$V'(\widetilde{q}) = V' + \frac{\epsilon}{2}\left(\frac{x - x_-}{\epsilon}\right)V'' + \mathcal{O}(\epsilon^2) \tag{C.8}$$

yields finally

$$\Delta H = \frac{\epsilon^3}{4}p\left[\frac{p^2}{6}V''' - V'V''\right] + \mathcal{O}(\epsilon^4). \tag{C.9}$$

This expression is the same as in Eq.(2.10), and hence the two formulations are identical.

D Conserved shadow quantity

A discretised Newtonian system is described by

$$x_+ + x_- - f(x) = 0. \tag{D.1}$$

Multiplying the above equation of motion by $(x_+ - x_-)$ results in

$$x_+^2 - x_-^2 - (x_+ - x_-)f(x) = 0 \quad \Rightarrow \quad x_+^2 - x_+ f = x_-^2 - x_- f. \tag{D.2}$$

The LHS of the right equation may be defined as $h(x_+, x) \widehat{=} x_+(x_+ - f)$. This is the function of x_+, x that is sought for translational symmetry. However, h might not be a conserved quantity going from $(x, x_-) \to (x_+, x)$ since the symmetry $h(x_+, x) = h(x, x_+)$ is not generally true.

However, the Newtonian system could potentially contain a conserved quantity if some function, $\widetilde{H}$, of (x_+, x) would equal the same function of (x, x_+). Such symmetric function in sought.

When attempting to construct $\widetilde{H}$, it could be assumed that this "shadow" Hamiltonian is a polynomial in h. A general polynomial in $h(x_+, x)$ is

$$A_0 + A_1 h + A_2 h^2 + \ldots = A_0 + A_1 x_+(x_+ - f) + A_2 x_+^2(x_+^2 - 2x_+ f + f^2) + \ldots, \tag{D.3}$$

where any possible x-dependance in coefficients A_n has been omitted for clarity.

Collecting terms of equal order in x_+ results in the above expression being equal to

$$A_0 + A_1 f x_+ + (A_1 + A_2 f^2)x_+^2 + \ldots. \tag{D.4}$$

From here, one may work to construct a symmetric function in x_+, x. For example, in the case of the harmonic oscillator, $A_0 + A_1 h$ is enough to construct $\widetilde{H}$ (see 2.3).

Unfortunately no symmetry was found within the scope of this report. It is expected not to exist such $\widetilde{H}$, since chaos is present [6].

E Chaotic behaviour in the q, p phase space

In this section, plots of the phase space spanned by the discrete variables q, p (Eq.(3.14)) are shown. Starting points for trajectories were randomly generated along the horizontal axis with $q \in [-1.9, 1.9]$ and $p = 0$.

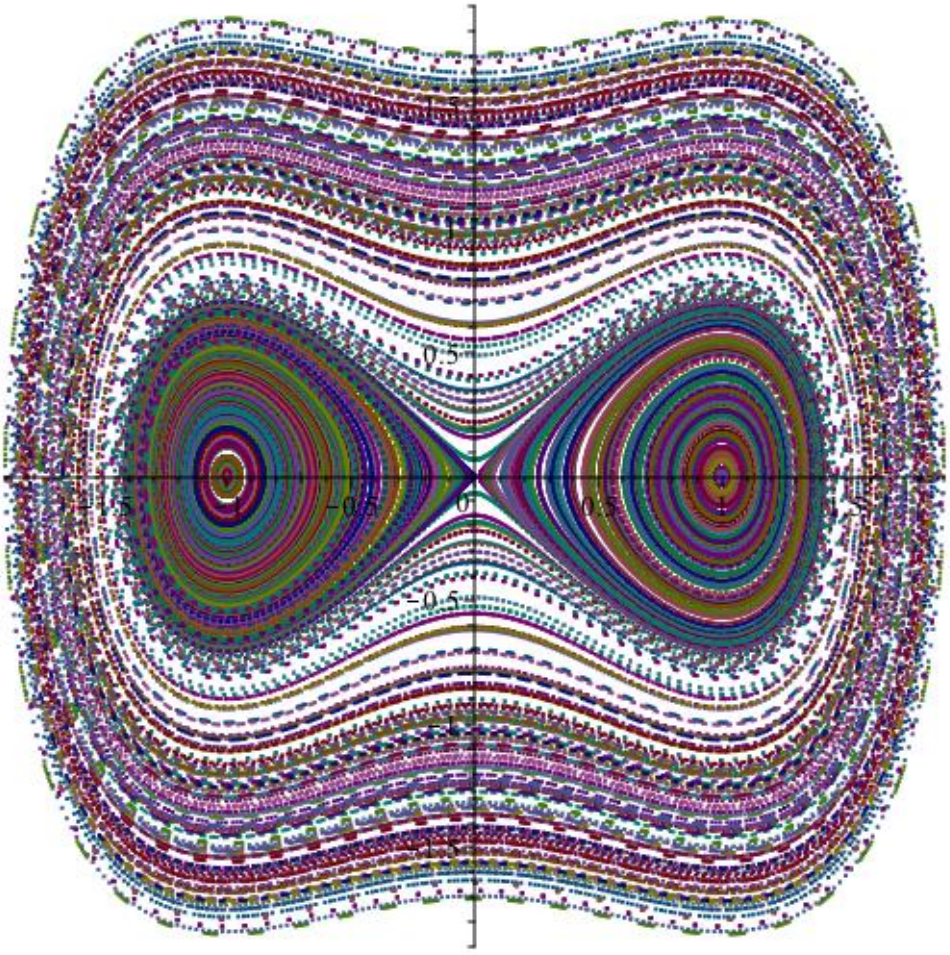

Figure 8: The figure displays the phase space spanned by the discrete variables q, p. $\epsilon = 0.1$ and chaos is insignificant.

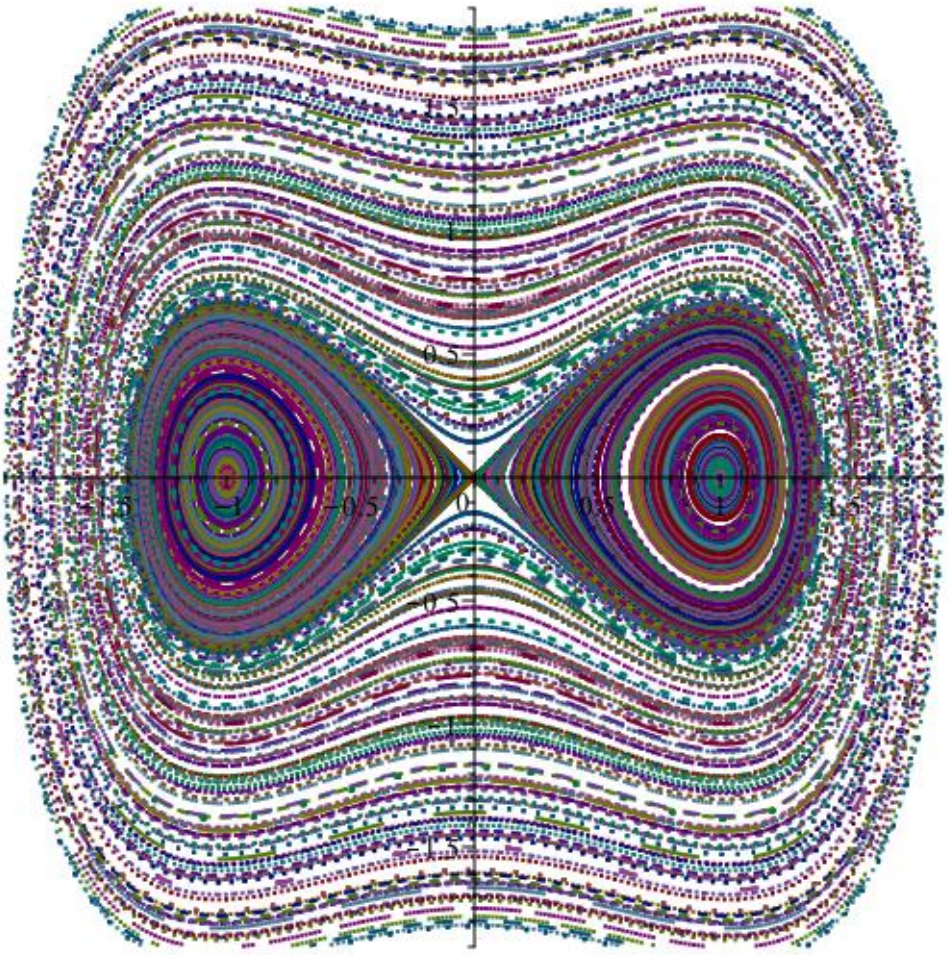

Figure 9: The figure displays the phase space spanned by the discrete variables q, p. $\epsilon = 0.3$ and chaos is insignificant.

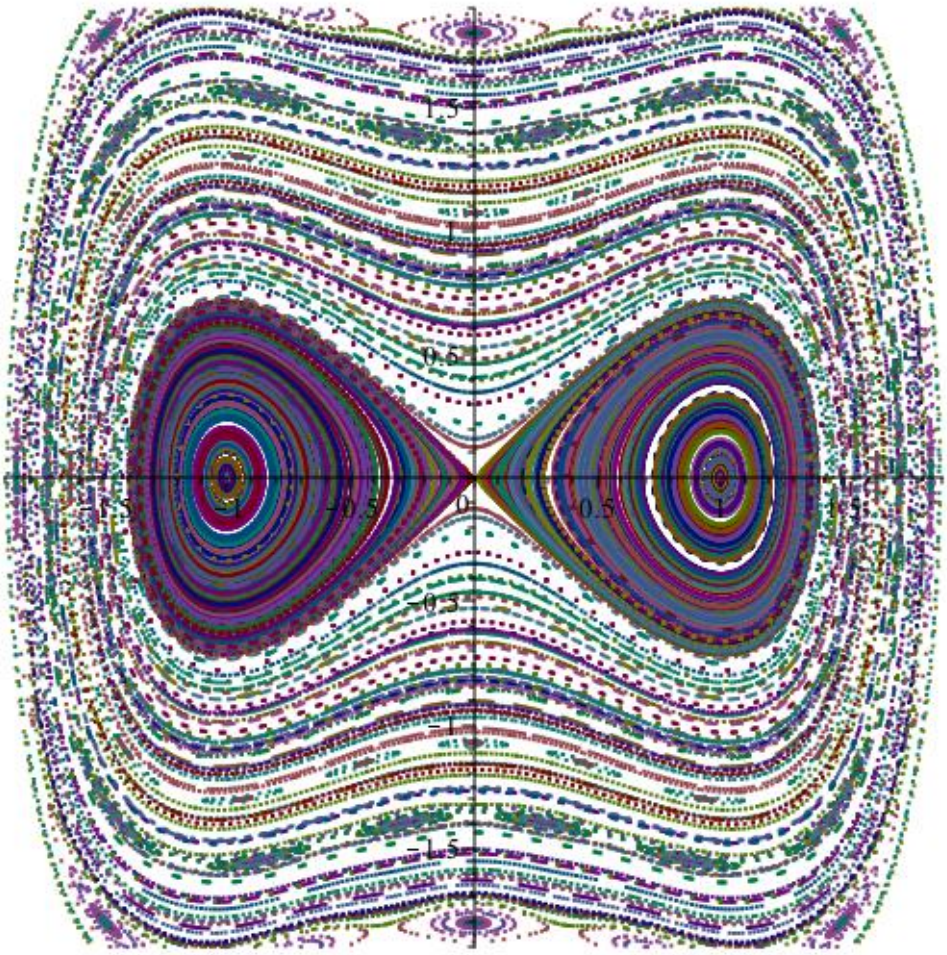

Figure 10: The figure displays the phase space spanned by the discrete variables q, p. $\epsilon = 0.4$ and chaotic behaviour can be seen along the borders of the plot with elliptic points emerging.

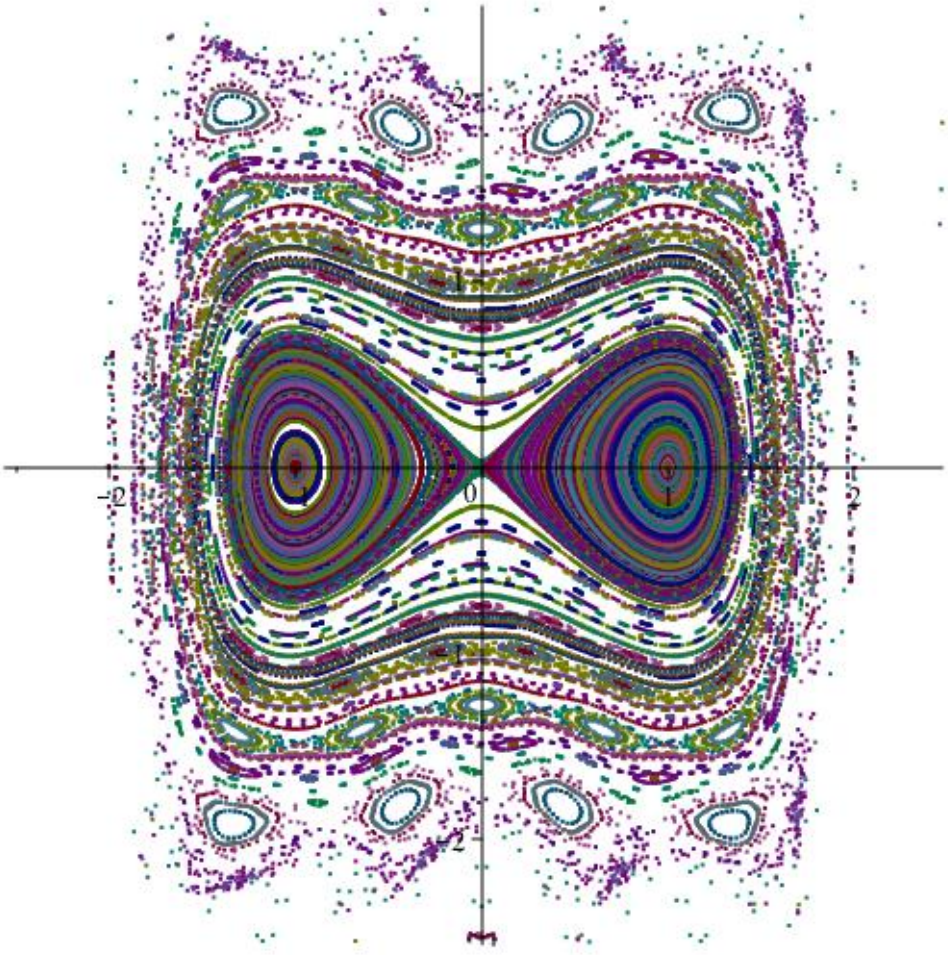

Figure 11: The figure displays the phase space spanned by the discrete variables q, p. $\epsilon = 0.48$ and chaotic behaviour can be seen along several trajectories with elliptic points emerging. At the origin, chaos can be seen as the region with trajectory points is opening up.

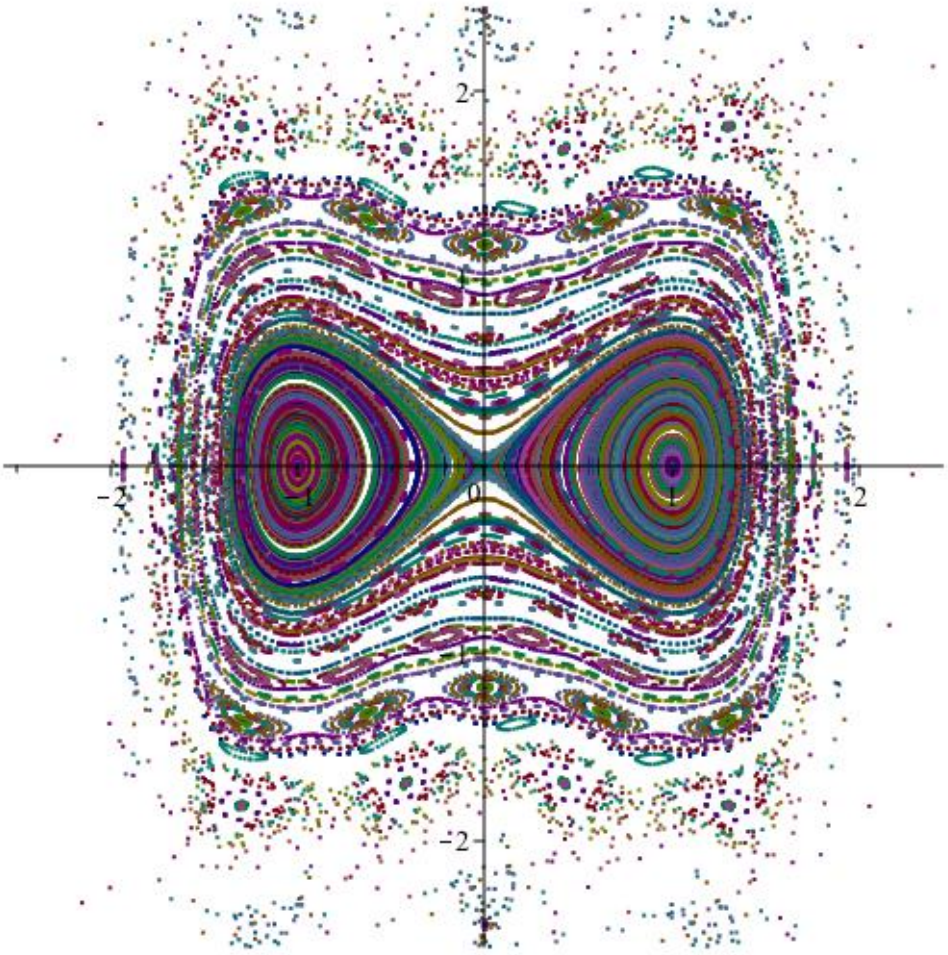

Figure 12: The figure displays the phase space spanned by the discrete variables q, p. $\epsilon = 0.5$ and chaotic behaviour is fairly obvious as the outer trajectories are breaking up. At the origin, chaos can be seen as the region with trajectory points is widening (c.f. Fig. 11).

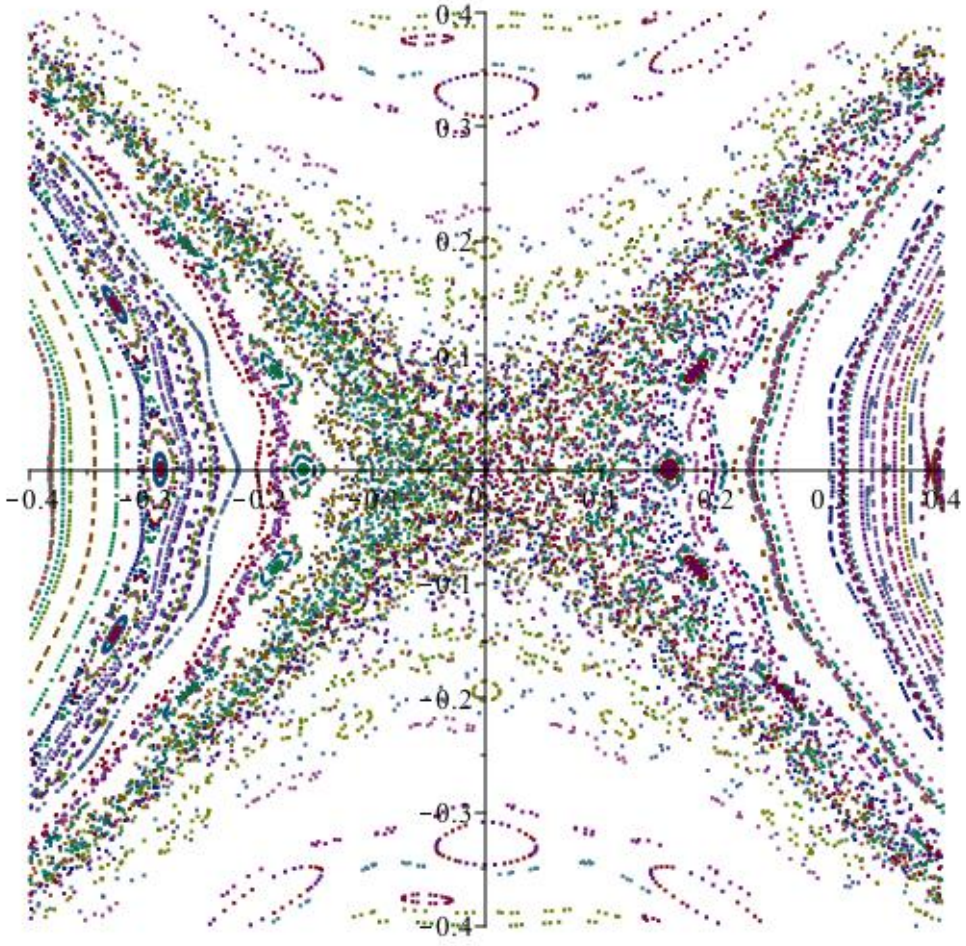

Figure 13: The figure displays a zoomed in view of the origin of the phase space spanned by the discrete variables q, p. $\epsilon = 0.55$. At the origin, chaos can be seen along with several elliptic points.

F Motion patterns

In this section, results are presented for the change in x as the spatial coordinate is updated in accordance with the map of Eq.(3.24).

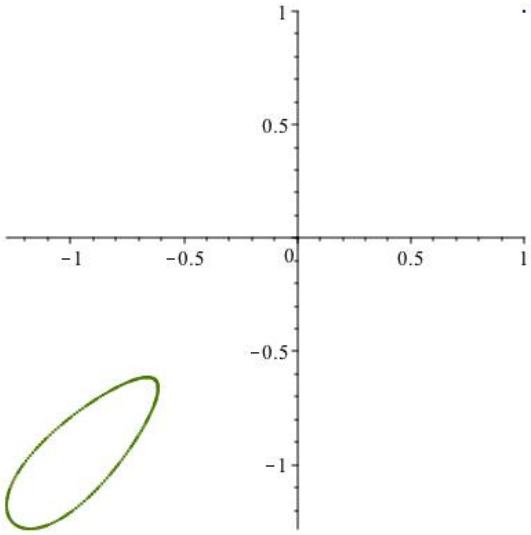

Figure 14: The figure shows a trajectory in phase space with a randomly generated starting point close to the elliptic fixed point with coordinates $(-1, -1)$. The curve has 250 points. $\epsilon = 0.5$.

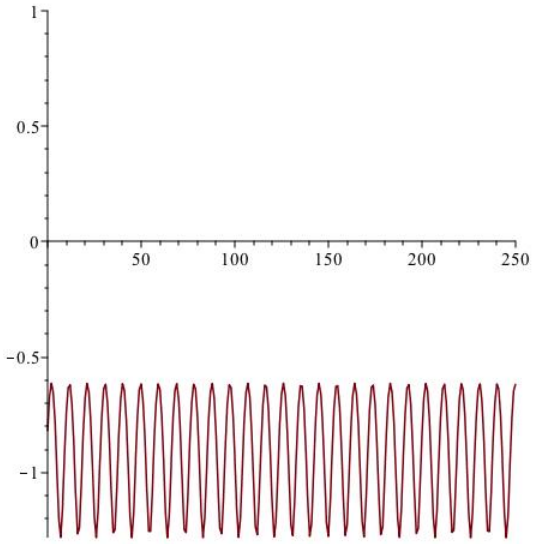

Figure 15: The figure shows oscillations in the spatial coordinate for motion along the trajectory of Fig. 14. The coordinate can be seen to oscillate around the value -1.

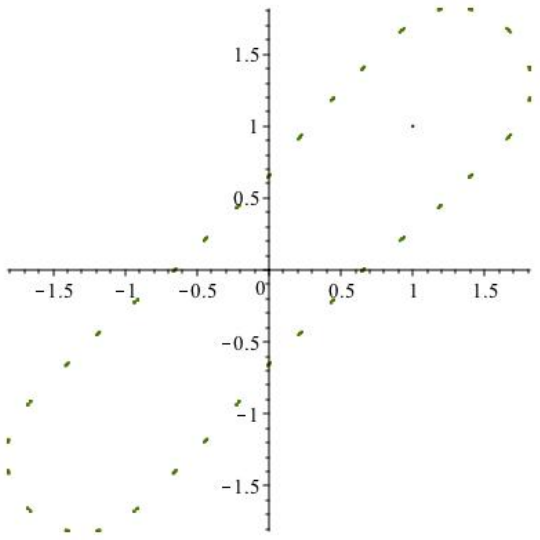

Figure 16: The figure shows a trajectory in phase space with a randomly generated starting point, far from the three main fixed points. The trajectory is very close to having a rational winding number. The curve has 250 points. $\epsilon = 0.5$.

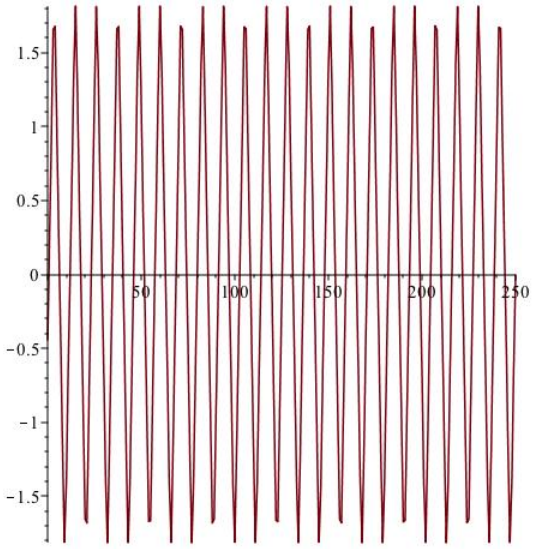

Figure 17: The figure shows oscillations in the spatial coordinate for motion along the trajectory of Fig. 16. The peaks in the diagram can be seen to oscillate in amplitude, with two higher peaks with a lower peak in between.

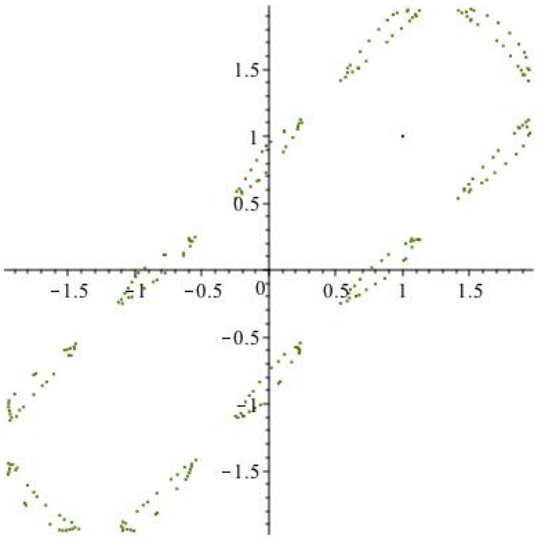

Figure 18: The figure shows a trajectory in phase space with a randomly generated starting point, far from the three main fixed points. The trajectory forms elliptic clusters around points on a trajectory with winding number 1/10 and therefore period 10. The curve has 250 points. $\epsilon = 0.5$.

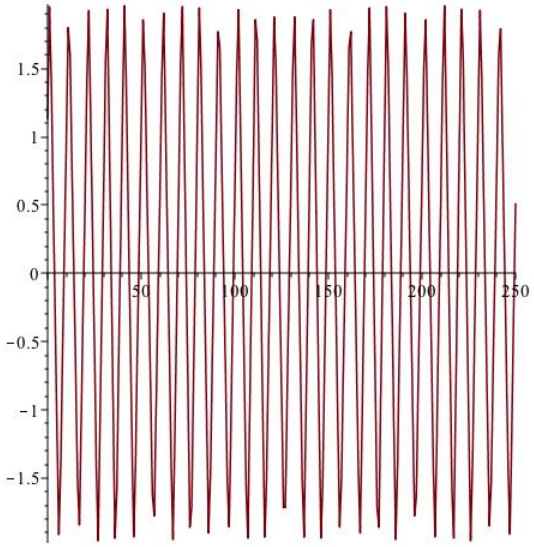

Figure 19: The figure shows oscillations in the spatial coordinate for motion along the trajectory of Fig. 18. The peaks in the diagram can be seen to oscillate in amplitude (c.f. Fig. 17).

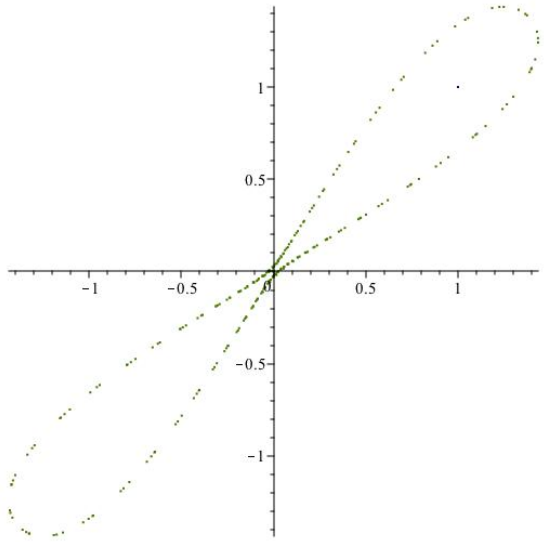

Figure 20: The figure shows a trajectory in phase space with a randomly generated starting point, close to the hyperbolic fixed point at the origin. The curve has 250 points. $\epsilon = 0.5$.

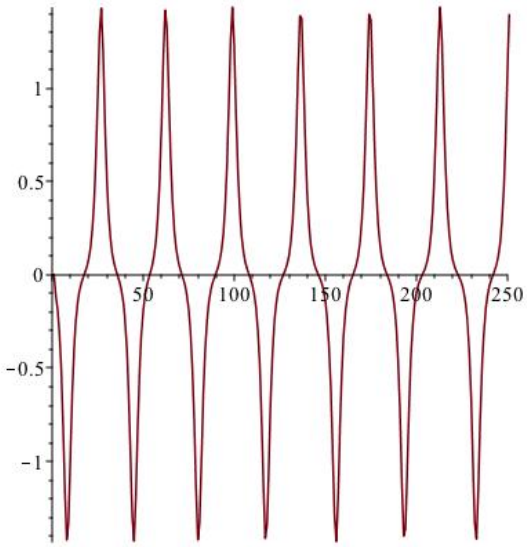

Figure 21: The figure shows oscillations in the spatial coordinate for motion along the trajectory of Fig. 20. The shape of the graph shows that motion is being slowed down close to the origin, before speed is increased again.

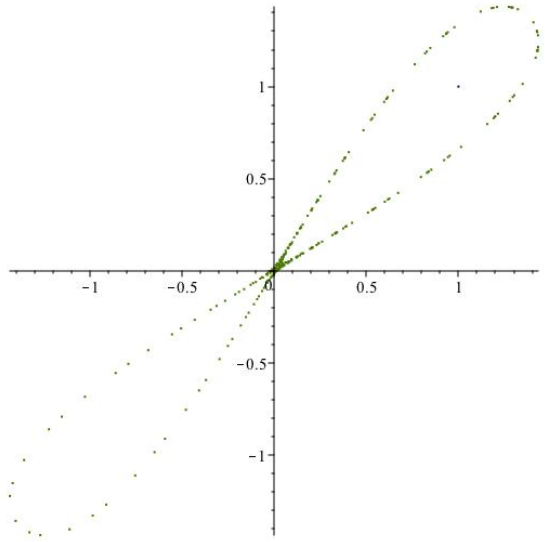

Figure 22: The figure shows a trajectory in phase space with a randomly generated starting point, experiencing chaotic movement close to the origin. The trajectory displays initial movement around both elliptic fixed points but after a while, chaos results in a closed path around one fixed point. The curve has 250 points. $\epsilon = 0.58$.

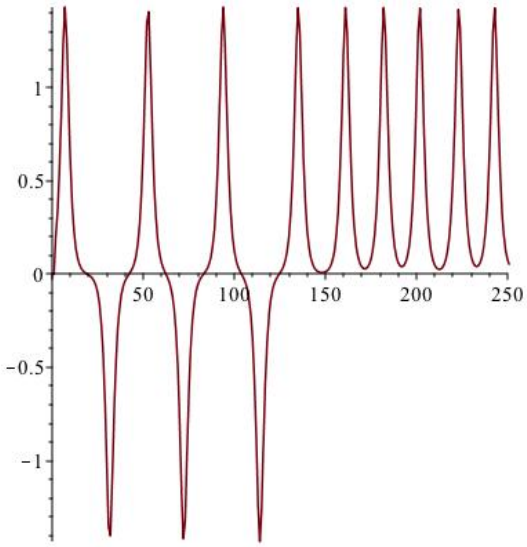

Figure 23: The figure shows oscillations in the spatial coordinate for motion along the trajectory of Fig. 22. As seen in the diagram, movement is initially symmetric around the origin. After about 100 steps, chaos at the origin forces movement in a different trajectory around the elliptic fixed point $(-1, -1)$. Here, oscillating amplitude can be seen, c.f Fig. 17 and Fig. 19.

Acknowledgements

There would never be any thesis published, if it was not for the supervisor. In this section, I would like to direct a big and sincere thank you to my supervisor, Bo Söderberg. Both for putting up with me, and for always being willing to teach with the goal of widening my knowledge, no matter the time of day or night. Thank you, Bosse. I have learnt a lot from you [6]!

References

[1] Vladimir Arnold. Proof of a theorem of A. N. Kolmogorov on the preservation of conditionally periodic motions under a small perturbation of the Hamiltonian. *Uspehi Mat. Nauk*, page 18, 1963.

[2] Niclas Blomberg. Undersökning av egenskaperna hos mönster i form av ickehomogena fixpunkter till en transportmodell. Student paper, LUP, June 2011.

[3] Andrey Kolmogorov. On the Conservation of Conditionally Periodic Motions under Small Perturbation of the Hamiltonian. *Dokl. Akad. Nauk SSR*, page 98, 1954.

[4] Jürgen Moser. On invariant curves of area-preserving mappings of an annulus. *Nachr. Akad. Wiss. Göttingen Math.-Phys. Kl. II*, pages 1–20, 1962.

[5] Patrik Sahlin, Bo Söderberg, and Henrik Jönsson. Regulated transport as a mechanism for pattern generation: Capabilities for phyllotaxis and beyond. *Journal of Theoretical Biology*, 258(1):60–70, 2009.

[6] Bo Söderberg. Private lectures and consultation, 2017.

[7] Anders Svensson. Periodiska fixpunkter till en modell av auxintransport, 2008.

[8] Jonathan Swinton, Erinma Ochu, and The MSI Turing's Sunflower Consortium. Novel Fibonacci and non-Fibonacci structure in the sunflower: Results of a citizen science experiment. *Royal Society Open Science*, 3(5), 2016.

[9] Nils Hermansson Truedsson. The Characteristics of Patterns in Simple Discrete Reaction-Diffusion Systems of Different Dimensionality and Number of Species. Student paper, LUP, 2014.